Worst-Case Analysis of Finite-Time Control Policies

David L. Ma and Richard D. Braatz

***Abstract*—Finite-time control policies are common in batch and semibatch operations. A novel approach is proposed that quantifies the impact of parameter and control implementation inaccuracies on the performance of such control policies. This information can be used to decide whether more experiments are needed to produce parameter estimates of higher accuracy, or to define performance objectives for the lower level control loops that implement the control trajectory. The approach is evaluated through application to the multidimensional growth of crystals used in nonlinear optics applications, where the nominal parameters and uncertainties are quantified from experimental data. Robustness estimates are provided with reasonable computational requirements.**

***Index Terms*—Batch control, crystallization, optimal control, robustness analysis, worst-case performance.**

I. Introduction

BATCH and semibatch processing are becomingly increasingly important with the rapid growth of the pharmaceutical and specialty chemicals industries. Finite-time control policies are common in batch and semibatch operations [45], [30], [13]. It has been observed that the product quality obtained from such finite-time trajectories can be highly sensitive to model parameter and control implementation uncertainties [33], [37]. For example, the mean crystal size in batch industrial crystallization processes can be highly sensitive to changes in temperature and in nucleation and growth kinetic parameters, all of which directly affect the tradeoff between crystal nucleation (which creates small crystals) and growth (which creates larger crystals). In this paper analysis tools are developed that assess the robustness of finite-time control policies to such uncertainties.

The model parameter and control implementation uncertainties are assumed to lie within a known bounded region. The analysis tools compute the worst-case deviation in the product quality (in optimal control, this is often called the cost functional) due to uncertainties. Also computed is a value for the uncertainties that result in the worst-case deviation in product quality. This information can be used to decide whether more laboratory experiments are needed to produce parameter estimates of higher accuracy, or to define performance objectives for lower level control loops which implement the control trajectory. The knowledge of the worst-case model parameter vector can be used to determine where experimental effort should be focused to improve model accuracy. The robustness analysis with regard to control implementation uncertainties can guide the selection of the control instrumentation, by determining where high-precision sensing and actuation are required. By expanding the control implementation uncertainty to explicitly include external disturbances, the computation of the worst-case external disturbances can determine which disturbances significantly affect the product quality and should be suppressed by redesign of the process or feedback control [24], [29], [50].

The analysis tools are applicable to processes that run for a finite time and satisfy a certain well-posedness property with respect to the control trajectory u and the model parameters θ. The well-posedness property is that the dependence of the product quality on deviations in the model parameters and the control trajectory can be accurately represented as a series expansion. A process that does not satisfy this property would be infinitely sensitive to perturbations in the control trajectory or the model parameters, in which case robustness analysis of the type discussed here would be unnecessary. Such a process may be poorly designed [4], in which case the process should be redesigned before any robustness analysis be considered.

This paper provides several extensions to the basic methodology developed for the case where the model parameters are assumed to lie within a hyperellipsoid [34]. One of the extensions is to handle uncertainties described by general Hölder norms. This more general representation includes the ∞-norm model uncertainty description usually considered in the chemical process design literature [4]. Also, this paper considers simultaneous model and implementation uncertainties for a finite-time system—we believe this is the first time this case has been treated within a worst-case formulation. The reason this is important is that it is possible for the product quality to be robust to model parameter uncertainties and control implementation uncertainties separately, while being nonrobust to simultaneous uncertainties of both types. The new algorithms are also able to incorporate higher order series expansions which in some cases may improve the accuracy of the calculated worst-case performance. Some of these results were presented at a conference [32].

The analysis tools are tested on a batch crystallization process, in which the product is a potassium dihydrogen phosphate crystal as would be used in nonlinear optics applications.

II. Mathematical Preliminaries

This paper uses the Hölder norm [25] defined by

$$\|v\|_p = (|v_1|^p + \cdots + |v_i|^p + \cdots + |v_n|^p)^{1/p}, \qquad p \geq 1. \quad (1)$$

When $p = \infty$

$$\|v\|_\infty = \max_i |v_i|. \quad (2)$$

Manuscript received March 9, 2000; revised September 15, 2000. Manuscript received in final form November 10, 2000. Recommended by Associate Editor F. Doyle. The work of D. L. Ma was supported by the Computational Science and Engineering Program. The work of R. D. Braatz was supported by the National Center for Supercomputing Applications.

The authors are with the University of Illinois at Urbana-Champaign, Urbana, IL 61801 USA (e-mail: braatz@uiuc.edu).

Publisher Item Identifier S 1063-6536(01)03369-3.

The following analysis also utilizes the induced Hölder norms:

$$||A||_{p,q} = \sup_{v \neq 0} \frac{||Av||_q}{||v||_p} = \max_{||v||_p \leq 1} ||Av||_q. \tag{3}$$

Analytical expressions for the induced Hölder norms for $(p, q) = (1, 1)$, $(2, 2)$, and (∞, ∞) are well known [25], while any combination of 1 and ∞ norms can be written as a linear program.

The notation $\dim(x)$ refers to the number of elements in the vector x.

III. Problem Formulation and Solution

The processes under consideration include nonlinear lumped or distributed parameter systems described by algebraic and intero-differential equations. For example, a lumped-parameter system may be described by the following set of differential and algebraic equations:

$$E\frac{dx}{dt} = f(x(t), u(t); \theta) \tag{4}$$

$$x(0) = x_0(\theta) \tag{5}$$

where

- x vector of state variables;
- u vector of control variables;
- θ vector of time-independent model parameters;
- E matrix of constant coefficients;
- f vector of algebraic relationships.

The differential-algebraic equations can include feedback control equations as well as equations for the physico-chemical phenomena. The product quality (i.e., cost functional) at a finite time t_f (e.g., at the end of a batch run) typically has the form

$$y(x(t), u(t); \theta) = g(x(t_f)) + \int_0^{t_f} F(x(t), u(t))\, dt. \tag{6}$$

The product quality y is a function of the states, the control trajectory, and the model parameters. While the focus of this paper is on processes in which the final time t_f is fixed, it is straightforward to generalize the approach so that t_f is treated as an uncertain parameter.

The goal is to derive expressions for the worst-case change in the product quality y that can occur for a bounded set of uncertainties in the model parameters θ and the control trajectory u. The approach uses a series expansion to quantify the product quality in a neighborhood around the control trajectory. This series expansion provides a mathematical simplification that will allow the derivation of analytical and semianalytical results for quantifying the worst-case product quality, and for computing the worst-case uncertainties. The series expansion only needs to be accurate for the operating region defined by the nominal control trajectory and the model and implementation uncertainty descriptions. This allows the use of a low number of terms in the expansion, even for highly nonlinear processes [33], [41]. After the robustness analysis is completed, the accuracy of series expansion evaluated at the worst-case estimates is assessed by comparing their values with those obtained by a nonlinear dynamic simulation using the predicted worst-case model parameters and control trajectory.

A. Uncertainty Description and Worst-Case Performance Formulation

Define $\hat{\theta}$ as the nominal model parameter vector of dimension $n \times 1$. Define $\delta\theta$ as the perturbation about the nominal model parameter vector, which is constrained in some uncertainty region. Then, the model parameter vector for the real system is

$$\theta = \hat{\theta} + \delta\theta. \tag{7}$$

Since we are interested in control algorithms which are implemented digitally, the nominal control trajectory can be represented as a vector $\hat{u}$ of dimension $m \times 1$. For example, a convenient representation for $\hat{u}$ for a temperature trajectory defined over fixed range of time could be the temperatures at m discrete time instances along the trajectory. In practice, nonminimum phase behavior, unknown process disturbances, and measurement noise cause performance limitations which result in an imperfect implementation of the control trajectory. Let δu be the perturbation about the nominal vector $\hat{u}$. Then, the control trajectory implemented on the process is

$$u = \hat{u} + \delta u \tag{8}$$

where δu is within a some specified region. It can be convenient for u to include a parameterization of disturbances among its elements [41]. This allows the analysis of the worst-case effect of disturbances on the performance objective y.

Two uncertainty descriptions are most used in the literature. One of these is the ellipsoidal description, in which case perturbations such as $\delta\theta$ are assumed to lie within the hyperellipsoid

$$\mathcal{E}_\theta = \{\theta\colon (\theta - \hat{\theta})^T V_\theta^{-1} (\theta - \hat{\theta}) \leq r^2(\alpha)\} \tag{9}$$

where

- V_θ $n \times n$ positive definite covariance matrix;
- α confidence level;
- r distribution function.

Uncertainty descriptions of this type are readily obtained by parameter estimation algorithms [2], [3], [14], [31]. Another representation for the model and implementation uncertainties is by independent bounds on each element [4]

$$\theta_{\min} \leq \theta \leq \theta_{\max} \tag{10}$$

$$u_{\min} \leq u \leq u_{\max}. \tag{11}$$

The Hölder norm is general enough to include both of these uncertainty descriptions. The sets of parameters and control trajectories including uncertainties can be represented as

$$\mathcal{E}_\theta = \{\theta\colon \theta = \hat{\theta} + \delta\theta,\ ||W_\theta \delta\theta||_p \leq 1\} \tag{12}$$

$$\mathcal{E}_u = \{u\colon u = \hat{u} + \delta u,\ ||W_u \delta u||_q \leq 1\} \tag{13}$$

where W_θ and W_u, are specified positive definite weighting matrices. Uncertainty descriptions (9)–(11) can be written in the general form (12) and (13). For example, (9) is written as (12) by setting $p = 2$ and $W_\theta = (1/r(\alpha))V_\theta^{-1/2}$. When there is some independent uncertainty in each model parameter, (10) is

written as (12) by setting $p=\infty$, $\hat{\theta}=(1/2)(\theta_{\max}+\theta_{\min})$, and W_θ as a diagonal matrix with diagonal elements defined by

$$(W_\theta)_{jj}=\frac{2}{\theta_{\max,\,j}-\theta_{\min,\,j}}. \tag{14}$$

In the next section, analytical expressions or computational algorithms are provided for computing the worst-case change in product quality and an associated worst-case parameter uncertainty and control trajectory. To be consistent with the robust control literature [58], henceforth the product quality y will be referred to as the *performance objective*. Define $\hat{y}$ as the performance objective when the system is operated under the nominal control trajectory $\hat{u}$ with the nominal model parameter $\hat{\theta}$, y as the performance objective when trajectory u and parameter vector θ are used, and the difference as $\delta y=y-\hat{y}$. The goal is to compute the worst-case performance

$$\max_{\substack{\|W_\theta\delta\theta\|_p\le 1\\ \|W_u\delta u\|_q\le 1}}|\delta y|. \tag{15}$$

To simplify the notation, the performance objective y will not be written as an explicit function of the states, that is,

$$y=y(u;\,\theta). \tag{16}$$

This is acceptable because the states are completely described as functions of the initial conditions x_0, the model parameters θ, and the control trajectory u [e.g., see (4)]. This notational simplification is commonly used in publications by the process optimization community [4].

B. Worst-Case Performance Evaluation

To simplify the presentation, the robustness analysis approach will be described in two sections. The first section uses a first-order series expansion which results in analytic expressions for the worst-case performance and the worst-case uncertainties. The second section describes the use of higher order series expansions, which results in higher accuracy but requires more computations.

1) First-Order Series Expansion: Assume that the deviation in performance δy can be described by first-order series expansion

$$\delta y=L\delta\theta+M\delta u. \tag{17}$$

For δy differentiable in $\delta\theta$ and δu, we have

$$L_i=\left.\frac{\partial u}{\partial\theta_i}\right|_{\theta=\hat{\theta},\,u=\hat{u}} \tag{18}$$

and

$$M_j=\left.\frac{\partial y}{\partial u_j}\right|_{\theta=\hat{\theta},\,u=\hat{u}}. \tag{19}$$

Similar well-posedness assumptions are regularly made in sensitivity analyzes for finite-time systems [15], [17], [28], [41], [43]. Such derivatives as well as higher order derivatives can be computed using divided differences [3] or by integrating the original algebraic-differential equations augmented with an additional set of differential-algebraic equations known as sensitivity equations [3], [9]. In particular, [9] lists the sensitivity equations for the dynamical system described by (4).

Using some matrix analysis, the worst-case performance is

$$\max_{\substack{\|W_\theta\delta\theta\|_p\le 1\\ \|W_u\delta u\|_q\le 1}}|L\delta\theta+M\delta u|=\|LW_\theta^{-1}\|_{p,\,r}+\|MW_u^{-1}\|_{q,\,r} \tag{20}$$

where r is equal to any integer. Now analytical expressions for the induced norms and the worst-case uncertainties are computed using Lagrange multipliers, where r is selected for convenience. For the case of $p=\infty$ and $q=1$

$$\|LW_\theta^{-1}\|_{p,\,r}=\|LW_\theta^{-1}\|_{\infty,\,\infty}=\|LW_\theta^{-1}\|_1 \tag{21}$$

and

$$\begin{aligned}\|MW_u^{-1}\|_{q,\,r}&=\|MW_u^{-1}\|_{1,\,1}=\|MW_u^{-1}\|_\infty\\&=\max_k|(MW_u^{-1})_k|\\&=|(MW_u^{-1})_{\overline{k}}|\end{aligned} \tag{22}$$

where a worst-case parameter uncertainty vector is[1]

$$\delta\theta_{w.c.}=W_u^{-1}v \tag{23}$$

with

$$v_k=\frac{(LW_\theta^{-1})_k}{|(LW_\theta^{-1})_k|} \tag{24}$$

and a worst-case implementation uncertainty vector is (see Footnote 1)

$$\delta u_{w.c.}=W_u^{-1}e \tag{25}$$

with

$$e_k=\begin{cases}1, & \text{for } k=\overline{k}\\ 0, & \text{for } k\ne\overline{k}.\end{cases} \tag{26}$$

Similar expressions hold for $p=1$ and $q=\infty$. A single general expression holds for p equal to any positive integer other than 1 or ∞

$$\|LW_\theta^{-1}\|_{p,\,r}=\left(\sum_{k=1}^{n}(|(LW_\theta^{-1})_k|)^{p/(p-1)}\right)^{(p-1)/p} \tag{27}$$

with the worst-case parameter uncertainty vector being (see Footnote 1)

$$\delta\theta_{w.c.}=W_\theta^{-1}v \tag{28}$$

where

$$v_k=\frac{(|(LW_\theta^{-1})_k|)^{1/(p-1)}}{\left(\sum_{k=1}^{n}(|(LW_\theta^{-1})_k|)^{p/(p-1)}\right)^{1/p}}. \tag{29}$$

Similar expressions hold for $\|MW_u^{-1}\|_{q,\,r}$ and the associated worst-case control implementation uncertainty vector.

[1]Another worst-case uncertainty vector is obtained by multiplying by minus one. While both vectors achieve the maximum deviation of $|\delta y|$, one of the vectors is associated with a worst-case increase in y while the other is associated with a worst-case decrease in y.

By using a series expansion [e.g., as in (17) and in the next section], the mathematical descriptions of the robustness analysis results are formulated independently of the specific mathematical representations for the systems equations and the performance objective. This allows the derivation of robustness results that apply whether or not the system includes algebraic or partial differential equations, or whether the system is continuous time or discrete time. The specifics of the dynamical system and the performance objective appear only in the calculation of L and M in (18) and (19). Some simulation programs have options for computing L and M with no additional input from the user [20], [36]. Sensitivities can be automatically computed even for hybrid discrete-continuous systems [23], [51].

2) Higher Order Series Expansions: Although first-order series expansions can provide high accuracy for many processes [41], for some processes improved accuracy is obtained by using higher order series expansions [33]. For example, a second-order series may be required to represent the dependence of δy on many of the elements of δu if the control trajectory is the solution of an optimal control problem. The higher order expansions are handled using generalizations of the structured singular value.

a) ∞-Norm uncertainty descriptions: We will first illustrate the approach for uncertainty sets (10) and (11), which are the most commonly used in the chemical process design [4] and robust process control literature [38], [48]. To simplify the expressions, first combine vectors θ and u into a new vector λ

$$\lambda = \begin{bmatrix} \theta \\ u \end{bmatrix} \tag{30}$$

with nominal value

$$\hat{\lambda} = \begin{bmatrix} \hat{\theta} \\ \hat{u} \end{bmatrix} \tag{31}$$

and perturbation

$$\delta\lambda = \lambda - \hat{\lambda} \tag{32}$$

$$a \le \delta\lambda \le b \tag{33}$$

where the vectors a and b are defined by the upper and lower bounds on the model parameters θ and the control trajectory u in (10) and (11).

First consider the case where it can be assumed that δy is accurately described by a second-order series expansion

$$\delta y = M_\lambda \delta\lambda + \delta\lambda^T H_\lambda \delta\lambda. \tag{34}$$

For δy twice differentiable in $\delta\lambda$, we have

$$(M_\lambda)_j = \left.\frac{\partial y}{\partial \lambda_j}\right|_{\lambda=\hat{\lambda}} \tag{35}$$

$$(H_\lambda)_{ij} = \left.\frac{\partial^2 y}{\partial \lambda_i \lambda_j}\right|_{\lambda=\hat{\lambda}}. \tag{36}$$

Then the analysis problem is to compute

$$\max_{a\le\delta\lambda\le b} |\delta y| = \max_{a\le\delta\lambda\le b} |M_\lambda \delta\lambda + \delta\lambda^T H_\lambda \delta\lambda|. \tag{37}$$

This problem can be rewritten in terms of the mixed structured singular value μ [19], [56], for which polynomial-time upper and lower bounds can be computed using off-the-shelf software [1]. For any real k

$$\max_{a\le\delta\lambda\le b} |M_\lambda \delta\lambda + \delta\lambda^T H_\lambda \delta\lambda| \ge k \Longleftrightarrow \mu_\Delta(N) \ge k \tag{38}$$

where

$$N = \begin{bmatrix} 0 & 0 & kw \\ kH_\lambda & 0 & kH_\lambda z \\ z^T H_\lambda + M_\lambda & w^T & z^T H_\lambda z + M_\lambda z \end{bmatrix} \tag{39}$$

$$w = \tfrac{1}{2}(b-a) \tag{40}$$

$$z = \tfrac{1}{2}(b+a) \tag{41}$$

and the perturbation block $\Delta = \mathrm{diag}(\Delta_r, \Delta_r, \delta_c)$, where Δ_r consists of independent real scalars and δ_c is a complex scalar [7], [8]. Thus the optimization problem (37) is given by

$$\max_{a\le\delta\lambda\le b} |\delta y| = \max_{\mu_\Delta(N)\ge k} k. \tag{42}$$

Upper and lower bounds for this problem can be computed by iterative μ-computations [38], but a more efficient way is to use skewed-μ, which requires no more effort than that required for a single μ calculation [18], [21], [49]. Polynomial-time upper and lower bound computations can be performed within a few minutes on a workstation for a problem with $\dim(u)+\dim(\theta) \le 100$, with the bounds usually being tight enough for engineering purposes [54]. The software computes a worst-case uncertainty vector as well as the worst-case performance [1].[2]

Now consider the case where it can be assumed that δy can be accurately described by a third-order series expansion

$$\delta y = M_\lambda \delta\lambda + \delta\lambda^T H_\lambda \delta\lambda + \sum_{i=1}^{n} \delta\lambda_i \delta\lambda^T B^i \delta\lambda \tag{43}$$

where $n = \dim(\lambda)$ and $\delta\lambda_i$ is the ith element of λ. For δy thrice differentiable in $\delta\lambda$, we have

$$B^i = \begin{bmatrix} \dfrac{\partial^3 y}{\partial\lambda_i \partial^2 \lambda_1^2} & \cdots & \dfrac{\partial^3 y}{\partial\lambda_i \partial\lambda_1 \partial\lambda_n} \\ \vdots & \ddots & \vdots \\ \dfrac{\partial^3 y}{\partial\lambda_i \partial\lambda_1 \partial\lambda_n} & \cdots & \dfrac{\partial^3 y}{\partial\lambda_i \partial^2 \lambda_n^2} \end{bmatrix}. \tag{44}$$

The analysis problem is to compute

$$\max_{a\le\delta\lambda\le b} |\delta y| = \max_{a\le\delta\lambda\le b} \left| M_\lambda \delta\lambda + \delta\lambda^T H_\lambda \delta\lambda + \sum_{i=1}^{n} \delta\lambda_i \delta\lambda^T B^i \delta\lambda \right|. \tag{45}$$

As before, this problem can be written in terms of the mixed structured singular value μ. Using the singular value decomposition, B^i can be decomposed into two lower dimensional matrices as

$$B^i = L^i_{n\times m_i} R^i_{m_i\times n} \qquad m_i \le n. \tag{46}$$

[2]See Footnote 1.

Applying similar block diagram algebra as used to derive (38) gives

$$\max_{a\le\delta\lambda\le b}\left|M_\lambda\delta\lambda+\delta\lambda H_\lambda\delta\lambda+\sum_{i=1}^{n}\delta\lambda_i\delta\lambda^T L^i R^i\delta\lambda\right|\ge k \iff \mu_\Delta(N)\ge k \quad (47)$$

where

$$N=\begin{bmatrix} kN_{11} & kN_{12}\\ N_{21} & N_{22}\end{bmatrix} \quad (48)$$

$$N_{11}=\begin{bmatrix} 0 & 0 & 0 & \cdots & 0\\ H_\lambda+\sum_{i=1}^{n}z_iB^i & 0 & L^1 & \cdots & L^n\\ w_1R^1 & 0 & 0 & \cdots & 0\\ \vdots & \vdots & \vdots & \vdots & \vdots\\ w_nR^n & 0 & 0 & \cdots & 0\end{bmatrix} \quad (49)$$

$$N_{12}=\begin{bmatrix} w\\ H_\lambda z+\sum_{i=1}^{n}z_iB^iz\\ w_1R^1z\\ w_2R^2z\\ \vdots\\ w_nR^nz\end{bmatrix} \quad (50)$$

$$N_{21}^T=\begin{bmatrix} M_\lambda^T+H_\lambda z+\sum_{i=1}^{n}z_iB^iz\\ w\\ (L^1)^{T_2}\\ \vdots\\ (L^n)^{T_2}\end{bmatrix} \quad (51)$$

$$N_{22}=M_\lambda z+z^TH_\lambda z+\sum_{i=1}^{n}z_iz^TB^iz \quad (52)$$

and the perturbation block is

$$\Delta=\text{diag}[\Delta_r,\,\Delta_r,\,\Delta_r^1,\,\ldots,\,\Delta_r^n,\,\delta_c] \quad (53)$$

where δ_c is a complex scalar, and each Δ_r and Δ_r^i are real matrices with the following structures:

$$\Delta_r=\text{diag}(\delta_1,\,\ldots,\,\delta_n) \quad (54)$$

$$\Delta_r^i=\text{diag}(\delta_i,\,\ldots,\,\delta_i) \quad (55)$$

with Δ_r^i being an $m_i\times m_i$ matrix. The optimization problem (45) is given by

$$\max_{a\le\delta\lambda\le b}|\delta y|=\max_{\mu_\Delta(N)\ge k}k. \quad (56)$$

As before, the right-hand side can be computed as a single skewed-μ calculation.

The N and Δ matrices for higher order expansions can be constructed automatically using software for multidimensional realization [46], [47]. The optimization problem is then given by the skewed-μ problem (56) with the constructed N and Δ matrices used in the μ-calculation. For the reaction and separations processes we have investigated, sufficient accuracy was obtained using a first-order or second-order expansion, so higher order expansions have been unnecessary.

b) Other uncertainty descriptions: Other Hölder norms on the uncertainty are handled in a similar manner, using the generalized structured singular value [5], [11], [12], [27], [55]. For the case where the deviation in the performance objective can be represented by second-order series expansion, the analysis problem is to compute

$$\max_{\substack{\|W_\theta\delta\theta\|_p\le1\\ \|W_u\delta u\|_q\le1}}|\delta y|=\max_{\substack{\|W_\theta\delta\theta\|_p\le1\\ \|W_u\delta u\|_q\le1}}|M_\lambda\delta\lambda+\delta\lambda^TH_\lambda\delta\lambda|. \quad (57)$$

Applying similar block diagram algebra as in the ∞-norm case gives

$$\max_{\substack{\|W_\theta\delta\theta\|_p\le1\\ \|W_u\delta u\|_q\le1}}|M_\lambda\delta\lambda+\delta\lambda^TH_\lambda\delta\lambda|\ge k\iff\mu_\Delta^*(N)\ge1 \quad (58)$$

where

$$N=\begin{bmatrix} 0 & 0 & kw\\ k(W_\lambda^{-1})^TH_\lambda W_\lambda^{-1} & 0 & 0\\ M_\lambda W_\lambda^{-1} & w^T & 0\end{bmatrix} \quad (59)$$

w is the vector of ones, $W_\lambda=\text{diag}(W_\theta,\,W_u)$, and the perturbation block $\Delta=\text{diag}(\Delta_r,\,\hat\Delta_r,\,\Delta_r,\,\hat\Delta_r,\,\delta_c)$ where Δ_r and $\hat\Delta_r$ are real matrices with the structures

$$\Delta_r=\text{diag}(\delta_1,\,\ldots,\,\delta_n) \quad (60)$$

$$\hat\Delta_r=\text{diag}(\delta_{n+1},\,\ldots,\,\delta_{n+m}) \quad (61)$$

and δ_c is a complex scalar.

In this case, the generalized structured singular value μ^* is defined to be zero if there is no Δ such that $\det(I-N\Delta)=0$, otherwise

$$\mu_\Delta^*=\left(\min_\Delta\{|||\Delta|||:\,\det(I-N\Delta)=0\}\right)^{-1} \quad (62)$$

where

$$|||\Delta|||\equiv\max\{\|\Delta_r\|_p,\,\|\hat\Delta_r\|_q,\,|\delta_c|\}. \quad (63)$$

The optimization problem (57) is given by

$$\max_{\substack{\|W_\theta\delta\theta\|_p\le1\\ \|W_u\delta u\|_q\le1}}|\delta y|=\max_{\mu_\Delta^*(N)\ge k}k. \quad (64)$$

The right-hand side can be computed as a single skewed-μ^* calculation. Polynomial-time upper and lower bounds for the generalized structured singular value are available [10]. Some of the upper and lower bounds are analytic, and with other upper bounds being written in terms of linear matrix inequalities which can be solved using publicly available software.

C. Improvement of Estimates

Series expansions are used to compute the worst-case performance and uncertainties. The accuracy of the series expansion evaluated at the worst-case estimates are assessed by comparing their values with those obtained by a nonlinear dynamic simulation using the estimated worst-case parameter vector. The values obtained by the nonlinear dynamic simulation are used as the final analysis estimates. This procedure will be illustrated in the following crystallization simulation.

IV. Application: Multidimensional Crystal Growth

Potassium dihydrogen phosphate (KDP, KH_2PO_4) crystals are important in nonlinear optics applications. The deuterated form of KDP is standard in commercial laser systems for frequency doubling from the near infrared to the visible [16]. KDP and DKDP ($K(D_xH_{1-x})_2PO_4$) crystals are currently the only nonlinear crystals which can be grown to the sizes needed for laser radiation conversion in laser fusion systems [42], [53], [57]. These nonlinear optics applications place high demands on the crystal quality, size, and quantity produced.

The KDP crystal shape is tetragonal prism in combination with tetragonal bipyramid and the angle between the prism sides and pyramid faces is 45° [39]. The two characteristic lengths r_1 and r_2 for a KDP crystal are shown in Fig. 1, and its volume is

$$v = (r_1 - r_2)r_2^2 + \tfrac{1}{3}\, r_2^3. \tag{65}$$

For nonlinear optic applications, each KDP crystal is grown from a single seed crystal in a batch of well-mixed solution in the metastable region (hence, no nucleation). Under these conditions, the habit of the KDP crystal is completely described by the growth rates in the r_1 and r_2 directions. The kinetic expressions of the growth rates obtained from experiments [39] are

$$\frac{dr_1}{dt} = \frac{k_{g1}}{\rho_c}\,(C - C_{\text{sat}})^2 \tag{66}$$

$$\frac{dr_2}{dt} = \frac{k_{g2}}{\rho_c}\,(C - C_{\text{sat}})^2 \tag{67}$$

where

ρ_c	density of the crystal ($= 2338$ kg/m^3);
C	solute concentration (kg of solute/kg of water);
C_{sat}	saturated solute concentration;
k_{g1} and k_{g2}	growth rate coefficients (kg/s m^2).

The growth rate coefficients are related to the temperature T by

$$k_{g1} = D_1 T + E_1 \tag{68}$$

$$k_{g2} = D_2 T + E_2. \tag{69}$$

The parameters D_1, D_2, E_1, and E_2 were determined from experimental data reported by [39]

$$D_1 = \hat{D}_1(1 + w_1), \qquad E_1 = \hat{E}_1(1 + w_1) \tag{70}$$

$$D_2 = \hat{D}_2(1 + w_2), \qquad E_2 = \hat{E}_2(1 + w_2) \tag{71}$$

where the nominal values for the parameters are given in Table I, and the parameter uncertainties are

$$-0.015 \le w_1 \le 0.015, \qquad -0.015 \le w_2 \le 0.015. \tag{72}$$

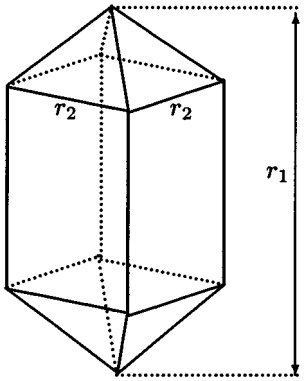

Fig. 1. Shape of KDP crystals.

TABLE I
Nominal Kinetic Parameters

$\hat{A}$ $\frac{\text{kg}}{\text{kg water °C}}$	0.0055
$\hat{B}$ $\frac{\text{kg}}{\text{kg water}}$	-1.384
$\hat{D}_1$ $\frac{\text{kg}}{\text{sec m}^2\ \text{°C}}$	0.101
$\hat{E}_1$ $\frac{\text{kg}}{\text{sec m}^2}$	-28.6
$\hat{D}_2$ $\frac{\text{kg}}{\text{sec m}^2\ \text{°C}}$	0.031
$\hat{E}_2$ $\frac{\text{kg}}{\text{sec m}^2}$	-8.35

The equilibrium solubility curve was also determined from experimental data reported by [39]

$$C_{sat} = AT + B \tag{73}$$

where

$$A = \hat{A}(1 + w_3), \qquad B = \hat{B}(1 + w_3) \tag{74}$$

the nominal values $\hat{A}$ and $\hat{B}$ are given in Table I, and

$$-0.02 \le w_3 \le 0.02. \tag{75}$$

The nominal values for the growth kinetics and solubility curve were determined by least-squares fitting, and the uncertainties were estimated from the deviations of the experimental data points from the best-fit curve.

When growing KDP crystals for nonlinear optics applications, the operating region of the crystallization is defined so as to avoid nucleation. This condition can be written as the constraint:

$$C - C_{\text{sat}} \le \Delta C_{\max}. \tag{76}$$

In practice, the KDP crystal is typically grown from one seed crystal in a batch of well-mixed solution which is cooled over a period of days [53]. A total mass balance directly links the solute concentration to the size of the crystal at any point during the process

$$C = C_0 + \frac{w_0}{m_{\text{solvent}}} - \frac{\rho_c v}{m_{\text{solvent}}} \tag{77}$$

where

C_0 initial concentration (kg solute/kg of water);
w_0 weight of the seed (kg solute);
m_{solvent} mass of the solvent (kg water).

The most common operating procedure when growing KDP crystals for use in nonlinear optics applications is to set the cooling temperature profile so as to try to keep the supersaturation $C - C_{\text{sat}}$ at its maximum value while satisfying concentration constraint (76) [57]. This maximizes the crystal growth rates (66) and (67) for each dimension, which maximizes the rate of crystal mass production. The desired nominal temperature trajectory is

$$\hat{T} = \frac{\hat{C} - \Delta C_{\max} - \hat{B}}{\hat{A}} \tag{78}$$

where $\hat{C}$ is the solute concentration measurement.

This temperature trajectory cannot be implemented exactly in practice for two reasons. First, the solute concentration measurement $\hat{C}$ can be biased from the true solute concentration C

$$\hat{C} = C(1 + w_4) \tag{79}$$

where

$$-0.001 \le w_4 \le 0.001. \tag{80}$$

Second, the temperature cannot be implemented exactly due to unmeasured disturbances (e.g., fluctuations in cooling water) and limitations to the performance of the local controller, hence the temperature actually achieved is

$$T = \frac{C(1 + w_4) - \Delta C_{\max} - \hat{B}}{\hat{A}} + \alpha t + \beta \tag{81}$$

with

$$-1.2\times10^{-7} \le \alpha \le 1.2\times10^{-7}, \qquad -0.01 \le \beta \le 0.01 \tag{82}$$

where the parameter β represents the accuracy of the local controller, and α accounts for an additional drift in temperature with time t. Implementation inaccuracies with this character have been observed in laboratory crystallizers [35]. The magnitude of the uncertainties in α and β were selected based on engineering judgment.

Habit modification for KDP crystals has been extensively studied (see, e.g., [40], [52], and the citations therein). The aspect ratio (r_1/r_2) is of importance for two-dimensional crystallization in general, and it is of interest to determine the robustness of the aspect ratio to the model and control implementation uncertainties.

The first step in the analysis was to numerically simulate the nominal model equations for the cooling KDP crystal growth process for the nominal temperature trajectory. Initial conditions and other physical parameters are given in Table II. The coefficients in the first series expansions used in the robustness analysis were computed by augmenting model equations with the sensitivity equations [9]. The coefficients for the second-order and third-order terms were computed by a combination of augmenting the model equations with the sensitivity equations and divided differences. The resulting system of equations was solved using the sparse ODE solver LSODES [26]. The analysis calculations were computed using MATLAB, with the μ calculations computed using the μ-Analysis and Synthesis Toolbox [1] at the highest level of accuracy for the upper and lower bounds, which were equal within the number of significant figures.

TABLE II
INITIAL CONDITIONS, FINAL CONDITIONS, AND SOME PARAMETERS

values	values
$r_1(t=0)$	0.001 m
$r_2(t=0)$	0.001 m
$T(t=0)$	305.2 °C
$C(t=0)$	0.335 kg solute/kg water
ΔC_{max}	0.04 kg solute/kg water
$m_{solvent}$	5 kg water
t_f	19 hr
$T(t=t_f)$	295.3 °C
$C(t=t_f)$	0.280 kg solute/kg water
$r_1(t=t_f)$	9.522 cm
$r_2(t=t_f)$	4.160 cm
$r_1(t=t_f)/r_2(t=t_f)$	2.289

Simulation and analysis results indicate that the aspect ratio can change by as much as 5% due to model and implementation uncertainties (see Table III). The uncertainties corresponding to the worst-case aspect ratio were the same for all series expansions (where "worst-case" was defined to be the largest aspect ratio, see Table IV). The worst-case performance estimates from the first-, second-, and third-order series were very close to the worst-case performance computed for the original nonlinear system with the worst-case uncertainties implemented. This is an additional confirmation of the accuracy of the series representations and the analysis tools.

The worst-case parameters can be understood in terms of the crystal growth kinetics. The derivative dr_1/dr_2 is

$$\frac{dr_1}{dr_2} = \frac{k_{g1}}{k_{g2}} = \frac{D_1T + E_1}{D_2T + E_2} = \left(\frac{w_1 + 1}{w_2 + 1}\right)\left(\frac{\hat{D}_1T + \hat{E}_1}{\hat{D}_2T + \hat{E}_2}\right). \tag{83}$$

An increase in w_1 or a decrease in w_2 increases dr_1/dr_2, which would be expected to lead to an increased aspect ratio r_1/r_2. According to (81), increases in w_4, α, or β result in an increase

TABLE III
NOMINAL AND WORST-CASE ASPECT RATIOS FROM THE FIRST-, SECOND-, AND THIRD-ORDER ANALYSES, AND FROM SIMULATION

	nominal	1^{st}	2^{nd}	3^{rd}	simulation
r_1/r_2	2.29	2.42	2.39	2.39	2.40

TABLE IV
PARAMETER VALUES CORRESPONDING TO THE WORST-CASE ASPECT RATIO

w_1	w_2	w_3	w_4	α	β
0.015	-0.015	0.02	0.001	1.2×10^{-7}	0.01

TABLE V
COMPUTATION TIMES FOR THE CONSTRUCTION OF THE SERIES EXPANSIONS AND FOR THE SUBSEQUENT ANALYSIS STEP (INDUCED NORM FOR FIRST-ORDER EXPANSION, μ ANALYSIS FOR SECOND- AND THIRD-ORDER EXPANSIONS)

	1^{st} order	2^{nd} order	3^{rd} order
Computation time	2 s	50 s	19 min

in temperature. By differentiating dr_1/dr_2 in (83) with respect to temperature T, it is seen that an increase in temperature also increases dr_1/dr_2. The relationship between w_3 and the aspect ratio is a bit more subtle. A plot of aspect ratio versus time indicates that the aspect ratio goes through a maximum at some intermediate time. An increase in w_3 decreases the crystal growth rates, resulting in proportionately less time spent during the low aspect ratio growth which occurs near the end of the batch run.

The computation times for the robustness analysis were quite reasonable (see Table V), considering the inherent computational complexity of exactly calculating the worst-case performance [8], [44], or even approximating the worst-case performance within a given ϵ [6], [22]. A minor modification on the theoretical proofs in [6] indicate that exact and ϵ-approximate worst-case analyses for the nonlinear processes considered here are at least as computationally challenging.

The computation time grows rapidly as a function of the order of the series expansion. Recall that the first-order analysis results are nearly equal to the exact results (see Table III), and in this case the added simulation time is a small fraction of the total simulation time, even when the sensitivity equations are not included. This means that the first-order robustness analysis can be incorporated within an optimization framework to design robust optimal control trajectories for batch and semibatch processes, without leading to an unreasonable increase in computational expense. The robustness analysis with the higher order expansions can be used at the very end of the robust optimal control synthesis to verify results, or can be embedded into the final stages of the optimization procedure to improve accuracy.

V. CONCLUSION

Algorithms were proposed that calculate the worst-case performance in batch and semibatch processing. The algorithms are the first to take into account both model and control implementation uncertainties. The algorithms are applicable to nonlinear lumped or distributed parameter systems. The utility of the algorithms was demonstrated in their application to a batch multidimensional crystallization process.

REFERENCES

[1] G. J. Balas, J. C. Doyle, K. Glover, A. K. Packard, and R. S. R. Smith, *μ-Analysis and Synthesis Toolbox (μ-Tools): Matlab Functions for the Analysis and Design of Robust Control Systems*. Natick, MA: The MathWorks, Inc., 1992.

[2] D. M. Bates and D. G. Watts, *Nonlinear Regression Analysis and Its Applications*. New York: Wiley, 1988.

[3] J. V. Beck and K. J. Arnold, *Parameter Estimation in Engineering and Science*. New York: Wiley, 1977.

[4] L. T. Biegler, I. E. Grossmann, and A. W. Westerberg, *Systematic Methods of Chemical Process Design*. Englewood Cliffs, NJ: Prentice-Hall, 1997.

[5] R. D. Braatz and O. D. Crisalle, "Robustness analysis for systems with ellipsoidal uncertainty," *Int. J. Robust Nonlinear Contr.*, vol. 8, pp. 1113–1117, 1998.

[6] R. D. Braatz and E. L. Russell, "Robustness margin computation for large scale systems," *Comput. Chemi. Eng.*, vol. 23, pp. 1021–1030, 1999.

[7] R. D. Braatz, P. M. Young, J. C. Doyle, and M. Morari, "Computational complexity of μ calculation," in *Proc. Amer. Contr. Conf.*. Piscataway, NJ: IEEE Press, 1993, pp. 1682–1683.

[8] ——, "Computational complexity of μ calculation," *IEEE Trans. Automat. Contr.*, vol. 39, pp. 1000–1002, 1994.

[9] M. Caracotsios and W. E. Stewart, "Sensitivity analysis of initial value problems with mixed ODE's and algebraic equations," *Comput. Chem. Eng.*, vol. 9, pp. 359–365, 1985.

[10] V.-S. Chellaboina, W. M. Haddad, and D. S. Bernstein, "Structured matrix norms for robust stability and performance with block-structured uncertainty," *Int. J. Contr.*, vol. 71, pp. 535–557, 1998.

[11] J. Chen, M. K. H. Fan, and C. N. Nett, "Structured singular values and stability analysis of uncertain polynomials—Part 1: The generalized μ," *Syst. Contr. Lett.*, vol. 23, pp. 53–65, 1994.

[12] ——, "Structured singular values and stability analysis of uncertain polynomials—Part 2: A missing link," *Syst. Contr. Lett.*, vol. 23, pp. 97–109, 1994.

[13] S. H. Chung, D. L. Ma, and R. D. Braatz, "Optimal seeding in batch crystallization," *Can. J. Chem. Eng.*, vol. 77, pp. 590–596, 1999.

[14] ——, "Optimal model-based experimental design in batch crystallization," *Chemometrics Intell. Lab. Syst.*, vol. 50, pp. 83–90, 2000.

[15] P. Courtin and J. Rootenberg, "Performance index sensitivity of optimal control systems," *IEEE Trans. Automat. Contr.*, vol. AC-16, pp. 275–277, 1971.

[16] B. Elvers, S. Hawkins, and G. Schulz, Eds., *Ullmann's Encyclopedia of Industrial Chemistry*, 5th ed. Deerfield Beach, FL: VCH, 1991, vol. A17, p. 549.

[17] A. H. Evers, "Sensitivity analysis in dynamic optimization," *J. Optimization Theory Applicat.*, vol. 32, pp. 17–37, 1980.

[18] M. K. H. Fan and A. L. Tits, "A measure of worst-case H_∞ performance and of largest acceptable uncertainty," *Syst. Contr. Lett.*, vol. 18, pp. 409–421, 1992.

[19] M. K. H. Fan, A. L. Tits, and J. C. Doyle, "Robustness in the presence of mixed parametric uncertainty and unmodeled dynamics," *IEEE Trans. Automat. Contr.*, vol. 36, pp. 25–38, 1991.

[20] W. F. Feehery, J. E. Tolsma, and P. I. Barton, "Efficient sensitivity analysis of large-scale differential-algebraic systems," *Appl. Numer. Math.*, vol. 25, pp. 41–54, 1997.

[21] G. Ferreres and V. Fromion, "Computation of the robustness margin with the skewed μ tool," *Syst. Contr. Lett.*, vol. 32, pp. 193–202, 1997.

[22] M. Fu, "The real structure singular value is hardly approximable," *Trans. Automat. Contr.*, vol. 42, pp. 1286–1288, 1997.

[23] S. Galan, W. F. Feehery, and P. I. Barton, "Parameter sensitivity functions for hybrid discrete-continuous systems," *Appl. Numer. Math.*, vol. 31, pp. 17–48, 1999.

[24] G. Gattu and E. Zafiriou, "A methodology for on-line setpoint modification for batch reactor control in the presence of modeling error," *Chem. Eng. J.*, vol. 75, pp. 21–29, 1999.

[25] G. H. Golub and C. F. van Loan, *Matrix Computations*. Baltimore, MD: Johns Hopkins Univ. Press, 1983.

[26] A. C. Hindmarsh, "ODEPACK, a systematized collection of ODE solvers," in *Scientific Computing*, R. S. Stepleman, Ed. Amsterdam, The Netherlands: North-Holland, 1983, pp. 55–64.
[27] S. H. Khatri and P. A. Parrilo, "Spherical mu," in *Proc. Amer. Contr. Conf.*. Piscataway, NJ: IEEE Press, 1998, pp. 2314–2318.
[28] E. Kreindler, "On performance sensitivity of optimal control problems," *Int. J. Contr.*, vol. 15, pp. 481–486, 1972.
[29] M. Krothapally, J. C. Cockburn, and S. Palanki, "Sliding mode control of I/O linearizable systems with uncertainty," *ISA Trans.*, vol. 37, pp. 313–322, 1998.
[30] Y. D. Lang, A. M. Cervantes, and L. T. Biegler, "Dynamic optimization of a batch cooling crystallization process," *Ind. Eng. Chem. Res.*, vol. 38, pp. 1469–1477, 1999.
[31] L. Ljung, *System Identification: Theory for the User*. Englewood Cliffs, NJ: Prentice-Hall, 1987.
[32] *Worst-case analysis of batch and semibatch control trajectories*. Dallas, TX, 1999, Paper 10A07.
[33] ——, "Worst-case performance analysis of optimal batch control trajectories," in *Proc. Europ. Contr. Conf.*, Aug.–Sept. 1999, IFAC. Paper F1011-2.
[34] ——, "Worst-case performance analysis of optimal batch control trajectories," *AIChE J.*, vol. 45, pp. 1469–1476, 1999.
[35] D. L. Ma, T. Togkalidou, and R. D. Braatz, "Multidimensional crystal growth from solution," in *AIChE Annu. Meet.*, Dallas, TX, 1999, Paper 03A02.
[36] T. Maly and L. Petzold, "Numerical methods and software for sensitivity analysis of differential-algebraic systems," *Appl. Numer. Math.*, vol. 20, pp. 57–79, 1996.
[37] S. M. Miller and J. B. Rawlings, "Model identification and control strategies for batch cooling crystallizers," *AIChE J.*, vol. 40, pp. 1312–1327, 1994.
[38] M. Morari and E. Zafiriou, *Robust Process Control*. Englewood Cliffs, NJ: Prentice-Hall, 1989.
[39] J. W. Mullin and A. Amatavivadhana, "Growth kinetics of ammonium- and potassium-dihydrogen phosphate crystals," *J. Appl. Chem.*, vol. 17, pp. 151–156, 1967.
[40] J. W. Mullin, A. Amatavivadhana, and M. Chakraborty, "Crystal habit modification studies with ammonium and potassium dihydrogen phosphate," *J. Appl. Chem.*, vol. 20, pp. 153–158, 1970.
[41] M. Nikolaou and V. Manousiouthakis, "Robust control of batch processes," in *Proc. Amer. Contr. Conf.* Piscataway, NJ: IEEE Press, 1988, pp. 665–670.
[42] J. Paisner, J. Boyes, S. K. W. Lowdermilk, and M. Sorem, "National ignition facility would boost US industrial competitiveness," *Laser Focus World*, vol. 30, pp. 75–77, 1994.
[43] D. W. Peterson, "On sensitivity in optimal control problems," *J. Optimization Theory Applicat.*, vol. 13, pp. 56–73, 1974.
[44] S. Poljak and J. Rohn, "Checking robust nonsingularity is NP-hard," *Math. Contr., Signals, Syst.*, vol. 6, pp. 1–9, 1993.
[45] J. B. Rawlings, S. M. Miller, and W. R. Witkowski, "Model identification and control of solution crystallization processes: A review," *Ind. Eng. Chem. Res.*, vol. 32, pp. 1275–1296, 1993.
[46] E. L. Russell and R. D. Braatz, "Model reduction for the robustness margin computation of large scale uncertain systems," *Comput. Chem. Eng.*, vol. 22, pp. 913–926, 1998.
[47] E. L. Russell, C. P. H. Power, and R. D. Braatz, "Multidimensional realizations of large scale uncertain systems for multivariable stability margin computation," *Int. J. Robust Nonlinear Contr.*, vol. 7, pp. 113–125, 1997.
[48] S. Skogestad and I. Postlethwaite, *Multivariable Feedback Control: Analysis and Design*. New York: Wiley, 1996.
[49] R. S. R. Smith, "Model validation for uncertain systems," Ph.D. dissertation, California Institute of Technology, Pasadena, 1990.
[50] T. Togkalidou and R. D. Braatz, "A bilinear matrix inequality approach to the robust nonlinear control of chemical processes," in *Proc. Amer. Contr. Conf.* Piscataway, NJ: IEEE Press, 2000, pp. 1732–1736.
[51] J. E. Tolsma and P. I. Barton, "Hidden discontinuities and parametric sensitivity calculations," SIAM J. Sci. Comput., 2000, submitted for publication.
[52] S. V. Verdaguer and R. R. Clemente, "Crystal growth of KDP from boiling solutions in the presence of impurities," *J. Crystal Growth*, vol. 79, pp. 198–204, 1986.
[53] S. Yang, G. Su, Z. Li, and R. Jiang, "Rapid growth of KH2PO4 crystals in aqueous solution with additives," *J. Crystal Growth*, vol. 197, pp. 383–387, 1999.
[54] P. M. Young, "Robustness with parametric and dynamic uncertainties," Ph.D. dissertation, California Institute of Technology, Pasadena, 1993.
[55] ——, "Robustness analysis with full-structured uncertainties," *Automatica*, vol. 33, pp. 2131–2145, 1997.
[56] P. M. Young, M. P. Newlin, and J. C. Doyle, "Practical computation of the mixed μ problem," in *Proc. Amer. Contr. Conf.* Piscataway, NJ: IEEE Press, 1992, pp. 2190–2194.
[57] N. P. Zaitseva, L. N. Rashkovich, and S. V. Bogatyreva, "Stability of KH_2PO_4 and $K(H,D)_2PO_4$ solutions at fast crystal growth rates," *J. Crystal Growth*, vol. 148, pp. 276–282, 1995.
[58] K. Zhou, J. C. Doyle, and K. Glover, *Robust and Optimal Control*. Englewood Cliffs, NJ: Prentice-Hall, 1995.